Modelling of rigid body dynamics with spatial frictional contacts

Grzegorz Kudra, Michał Szewc, Michał Ludwicki, Krzysztof Witkowski, Jan Awrejcewicz

Abstract: The work focuses on a special class of reduced models of resultant friction forces coupled with rolling resistance for finite size of contact area and their applications in modelling and effective numerical simulations of spatial rigid body dynamics. The contact models are based on the integral expressions assuming fully developed sliding and Coulomb's friction law at each element of a finite contact zone. The integral models are then approximated by special functions, more effective in numerical simulations. The contact models are applied in different configurations of a spatial pendulum with Cardan joints, equipped with a special movable obstacle situated below the pendulum and limiting the space of admissible positions of the system. The models are tested numerically during investigations of bifurcation dynamics of the pendulum as well as a special experimental rig is prepared for their experimental validation.

1. Introduction

In many fields of science like mechanical engineering, mechatronics, robotics or control theory there are systems which consists of pendulums or multi-pendulums. They often play a significant role in system dynamics and may lead to interesting bifurcation phenomena. Analyzing the systems with pendulums, one can encounter models with spatial pendulums with a leading example, which is a single spherical pendulum and its different configurations [1,2]. The other more complex system, which is a spatial multi-dimensional pendulum is much less frequent object of interest and scientific analysis concerning pure non-linear dynamics [3]. The reason for the lack of works in this area may be the complexity of the system and its analysis.

Another important part of the analysis of a mechanical system is the friction and impact investigation. Both above mentioned components of the system play a significant role in changing bifurcation dynamics. Therefore, their investigation and developing new methods of analysis should be one of the most important steps in mechanical system study. On the other hand, new developed methods should lead to fast and reliable numerical simulations of the analyzed mechanical system. For this reason it is necessary to validate the numerical results with the real object measurements. In this case, not only the friction forces distribution is important, but modelling of impact in 3D space as well.

However, the analysis of full contact problem may result in high computational cost and a need to use such methods as finite element method. Therefore, the simplified or reduced models may be introduced.

An example of such approach is presented in the paper of Contensou [4], where one can find an integral model of friction force for fully developed sliding on a circular contact area. Another example may be found in the work of group of researches, who developed special group of approximations of the integral model friction [5], which allows to avoid integration over the contact area. Special approximations were presented for different shapes of the contact, not only the circular one [6]. An exemplary usage of the introduce approximations was presented in the numerical simulations of wobblestone, billiard ball and full ellipsoid of revolution [7-9].

This paper presents the mechanical system consisting of the double spatial pendulum with a spherical end of the second pendulum's limb, which can be in contact with a movable obstacle. This work is the collection of elements of the previous works [3, 6-10] with the continuation by new experimental rig development and further analysis of the system of double spatial pendulum with obstacle. The friction force is modelled in the similar way as presented in works [6-9], while Hertz stiffness with special model of damping [11] is used for normal force modelling.

Section 2 of this paper presents the model of the pendulum and the special laboratory stand for the results verification. In section 3 the numerical analysis of the system is presented. The summary and conclusions are drawn in section 4.

2.   Mathematical model

The analyzed mechanical system is the double spatial pendulum with a solid ball at the end of second limb. The ball can be in contact with a rotating obstacle. The physical model and its application in an experimental rig is presented in Fig. 1. The center O_1 of the global coordinate system O_1xyz is situated at the geometric center of the first massless Cardan-Hook joint. The joint connects the first element (body 1 of mass m_1) of the pendulum with the body 0. The body 0 is connected to the DC motor, which generates the rotational motion of the body 0, with angular position represented by angle ψ_1. Since the next coordinate system $O_1x_1y_1z_1$ is fixed with respect to the body 1, the angular position of the first limb of pendulum may be represented by the following sequence of rotations: by angle ψ_1 about axis z_1, by angle θ_1 about axis x_1 and by angle φ_1 about axis y_1. It is assumed that for each rotation angle equal to zero, the two coordinate systems $O_1x_1y_1z_1$ and O_1xyz overlap each other.

The second element (limb 2 with mass m_2) of the pendulum is connected to the first one by the identical massless Cardan-Hook joint. The centre O_2 of the joint lies on the axis O_1z_1 and its position is defined by the parameter $L_1= O_1O_2$. The similar sequence of rotations is used to describe angular position of the second limb: by angle θ_2 about axis y_2 and by angle φ_2 about axis z_2 of the body 2 – fixed coordinate system $O_2x_2y_2z_2$, with the centre at the point O_2. It is assumed that the coordinate system

$O_2x_2y_2z_2$ has the parallel axes to the corresponding ones of the coordinate system $O_1x_1y_1z_1$ for θ_2 and φ_2 equal to 0.
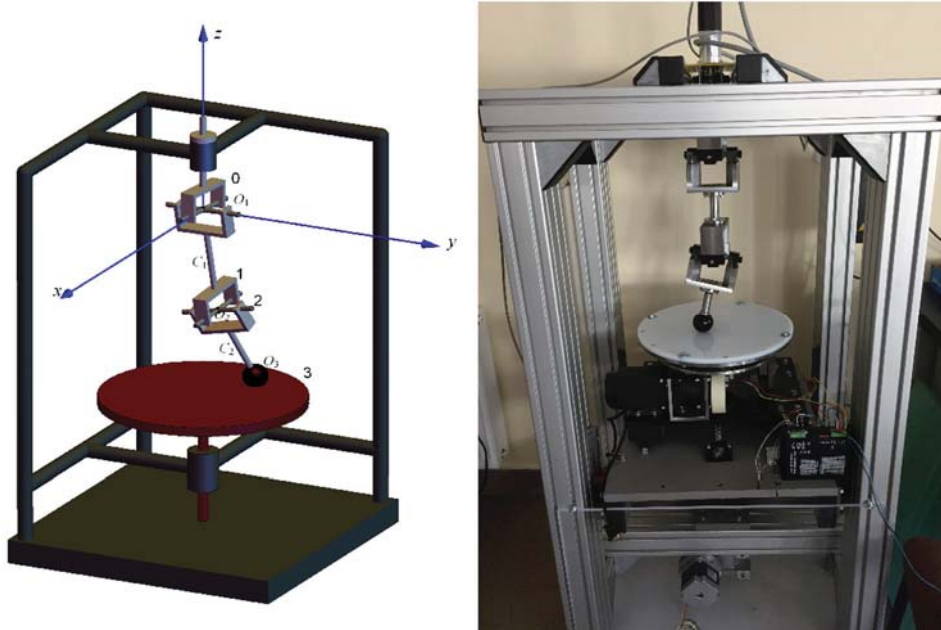
Figure 1. The double spatial pendulum with movable obstacle – model and experimental rig.

The ball at the end of second limb of pendulum, which can contact the movable obstacle 3, has a radius R_b and is centered at the point O_3 lying on the axis O_2z_2. The position of the center of the ball is described by the parameter $L_2= O_2O_3$. The assumption has been made, that the mass centres of both links of pendulum (C_1 and C_2) lie on the corresponding axes O_1z_1 or O_2z_2. Parameters $e_1= O_1C_1$ and $e_2= O_2C_2$ define positions of the mass centres. Additionally, the coordinate systems $O_1x_1y_1z_1$ and $O_2x_2y_2z_2$ are the principal axes of inertia of the corresponding bodies. Finally their mass distribution are defined by six parameters I_{xi}, I_{yi} and I_{zi} ($i=1,2$), which describes the principal central moments of inertia of the corresponding bodies with respect to the axes parallel to the corresponding axes O_ix_i, O_iy_i or O_iz_i. The last body in the mechanical system analysed is the rotating disk 3. Its rotation about the axis z of the global coordinate system is defined by the velocity ω_d. Moreover, the disk can change its horizontal position, which is described by the parameter z_0 - the coordinate of any point of the disk's surface along the axis z.

Based on the physical model described above, the experimental rig was made, which is presented in Fig. 1. It consists of exactly the same elements as presented in the physical model - body 0, limbs 1 and 2 and movable obstacle 3. To provide the rotational movement of the body 0 the highly dynamic

DC servo drive with integrated 4Q servo controller is used. It is equipped with incremental encoder with a resolution of 1024 pulses per revolution. To measure the movement of the pendulum limbs, there are two separate internal measurement units, which combine a 3-axis gyroscope and a 3-axis accelerometer on each board. Sensors are communicating with the processor by I2C bus and all wirings are made through the slip ring. The transmission between its stator and rotor takes place via sliding contacts, which allows the data to be transferred to the processor.

Mathematical model of the system is based on the work [10] and is expressed using the Lagrange's formalism

$$\frac{d}{dt}\left(\frac{\partial T}{\partial \dot{\theta}_i}\right) - \frac{\partial T}{\partial \theta_i} + \frac{\partial V}{\partial \theta_i} = Q_{\theta_i}\,, \quad \frac{d}{dt}\left(\frac{\partial T}{\partial \dot{\varphi}_i}\right) - \frac{\partial T}{\partial \varphi_i} + \frac{\partial V}{\partial \varphi_i} = Q_{\varphi_i}\,, \quad i=1,\,2 \tag{1}$$

where angles θ_i and φ_i $(i=1,2)$ are chosen as generalized co-ordinates and T denotes kinetic energy, V – is potential energy of gravity forces, Q_{θ_i} and Q_{φ_i} $(i=1,2)$ – the corresponding generalized forces. It is assumed that the pendulum is driven by the angular velocity of the body 0 defined by the following function of time

$$\omega(t) = \omega_0 + q\cos(\Omega t)\,. \tag{2}$$

The generalized forces are divided into the parts $Q_{\xi_{ic}}$ $(\xi = \theta, \varphi;\ i=1,2)$ representing the contact forces and $Q_{\xi_{ib}}$ representing damping in the joints:

$$Q_{\xi i} = Q_{\xi ic} - Q_{\xi ib}\,. \tag{3}$$

Resistance in the joints is modelled in the following way

$$Q_{\xi_i b} = M_b\,\frac{\dot{\xi}_i}{\sqrt{\dot{\xi}_i^2 + \varepsilon_b^2}}\,, \quad \xi = \theta, \varphi, \quad i=1,2 \tag{4}$$

where M_b is magnitude of the resistance torque common for all the joints and ε_b is parameter, which initially was assumed to be small and played a role of regularization of non-smooth sign function. But during different experiments performed by the authors, it occurred that the function (4) with higher values of ε_b can lead to better modelling of resistance in rolling bearings working in similar dynamical systems.

The generalized contact forces $Q_{\xi_i c}$ are related to the reaction $\mathbf{F}_c = \mathbf{N} + \mathbf{T}$ of the obstacle acting on the ball in following way

$$Q_{\xi_i c} = (\mathbf{N} + \mathbf{T}) \cdot \frac{\partial \mathbf{r}_{A_2}}{\partial \xi_i}, \quad \xi = \theta, \varphi, \quad i = 1,2 \tag{5}$$

where vector $\mathbf{r}_{A_2}$ indicates the position in the co-ordinate system O_1xyz of the point A_2 being the body's 2 fixed point taking temporarily the position of the circular contact zone center, while $\mathbf{N}$ and $\mathbf{T}$ are normal and tangent components of the reaction, respectively.

Normal component of the impact force is modelled based on the Hertzian contact stiffness and damping [11]

$$\mathbf{N} = N\mathbf{n} \tag{6}$$

where

$$N = \begin{cases} |h|^{3/2} k \left(1 - b\dot{h}\right) & \text{for } h \leq 0 \text{ and } 1 - b\dot{h} \geq 0 \\ 0 & \text{for } h > 0 \text{ or } 1 - b\dot{h} < 0 \end{cases} \tag{7}$$

where $\mathbf{n}$ is unit vector normal to the obstacle, h is distance between the ball and the surface of the disk, k is stiffness and b is damping coefficient of the contact.

For the contact of a ball of radius R_b with an elastic semi-space one gets based on the Hertz's theory

$$k = \frac{4\sqrt{R_b}}{3\left(\dfrac{1 - \nu_1}{E_1} + \dfrac{1 - \nu_2}{E_2}\right)}, \tag{8}$$

where ν_1 and ν_2 are Poisson's coefficients, while E_1 and E_2 are Young's modulus of the materials of the contacting bodies.

Friction force $\mathbf{T}$ is modelled based on assumption of fully developed sliding and Coulomb friction model valid at each point of the circular contact area with circularly symmetric contact pressure distribution. The corresponding integral model is approximated using special function of the following form [6-9]

$$\mathbf{T} = -\mu N \frac{\mathbf{v}_s}{\sqrt{\mathbf{v}_s^2 + b_T^2 a_r^2 \boldsymbol{\omega}_s^2 + \varepsilon^2}}, \tag{9}$$

where μ is friction coefficient, $\mathbf{v}_s$ and $\boldsymbol{\omega}_s$ are translational and angular sliding relative velocities at the center of the contact, a_r – radius of the contact calculated based on the Hertz theory and depending on the current normal loading of the contact, b_T – parameter depending on the contact stress distribution and ε – the parameter introduced in order to regularize function (9) and avoid singularity for vanishing relative motion of the contacting bodies.

3. Numerical simulations

The following values of the parameters were obtained based on materials and geometric shapes of the corresponding parts of the real pendulum being under preparation: $m_1 = 4.59$ kg, $m_2 = 2.41$ kg, $I_{x1} = I_{y1} = 0.0315$ kg·m², $I_{z1} = 0.0078$ kg·m², $I_{x2} = 0.0084$ kg·m², $I_{y2} = 0.0055$ kg·m², $I_{z2} = 0.0038$ kg·m², $L_1 = 0.228$ m, $L_2 = 0.175$ m, $e_1 = 0.122$ m, $e_2 = 0.0586$ m, $R_b = 0.025$ m. Additionally the following set of parameters is assumed to be constant during the subsequent numerical simulations as well: $g = 9.81$ m/s², $M_b = 0.04$ N·m, $\varepsilon_b = 0.4$, $v_1 = v_2 = 0.3$, $E_1 = 2 \cdot 10^9$ N/m², $E_2 = 0.1 \cdot 10^9$ N/m², $b = 0.5$ m⁻¹s, $z_0 = -425$mm , $\mu = 0.2$, $\omega_d = 0$ rad/s , $\omega_0 = 0$ rad/s , $q = 5$ rad/s , $\Omega = 5$ rad/s and $\varepsilon = 10^{-3}$ m/s (except the cases where one of them is chosen as bifurcation parameter).

Figure 2 presents bifurcation diagrams with angular frequency of the obstacle ω_d playing a role of control parameter. Bifurcation diagrams are made for two cases: with the parameter $b_T = 0.681$ (a) corresponding to circular contact with Hertzian stress distribution and with $b_T = 0$ (b), i.e. for the case of a point contact and no relation between friction force and rotational relative motion of the contacting surfaces.


a)

b)
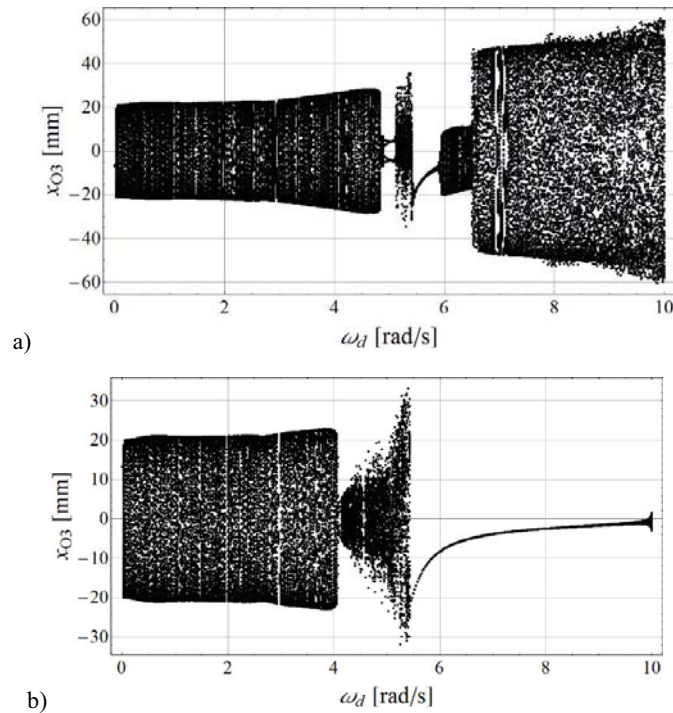
Figure 2. Bifurcation diagrams of the system with angular frequency of the obstacle ω_d as a control parameter, for $b_T = 0.681$ (a) and $b_T = 0$ (b)

Results of further analysis of the influence of the model (9) on the system dynamics is presented in Fig. 3, on bifurcation diagram, where as a control parameter is chosen coefficient b_T. One can observe a significant role in bifurcation dynamics of the pendulum played by the contact pressure distribution. Next pair of bifurcation diagrams is exhibited in Fig. 4, where the friction coefficient μ is chosen as a bifurcation parameter. Fig. 5 and Fig. 6 exhibits bifurcation diagrams with position of the obstacle z_0 varying quasi-statically from -428 mm to -417 mm. Note that for $z_0 \leq z_0^* = -L_1 - L_2 - R_b = -427\,\text{mm}$ the obstacle is below the range of the pendulum and for the assumed parameters the system tends to the stable fixed point with $\theta_1 = \varphi_1 = \theta_2 = \varphi_2 = 0$. For $z_0 = z_0^*$ one observe collision of this equilibrium position with the limiter of motion. Further increase of height of the obstacle leads to complex bifurcation dynamics. Fig. 5 is the bifurcation diagram for $b_T = 0.681$ and Fig. 6 is the bifurcation diagram for $b_T = 0$.
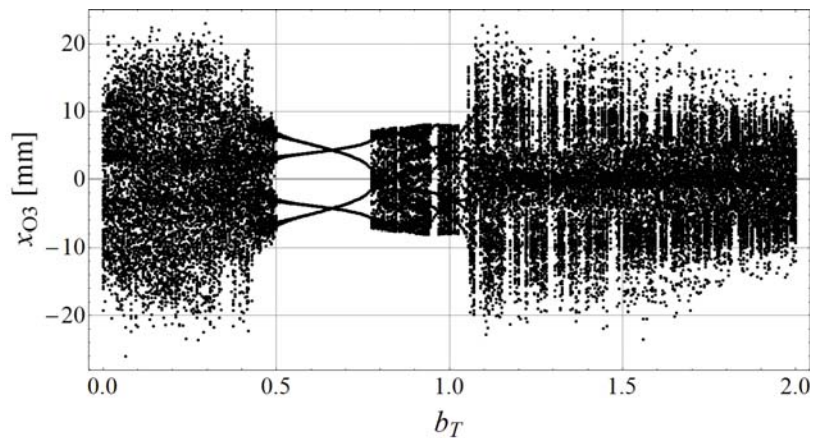
Figure 3. Bifurcation diagram of the system with the coefficient b_T of the contact model as a control parameter
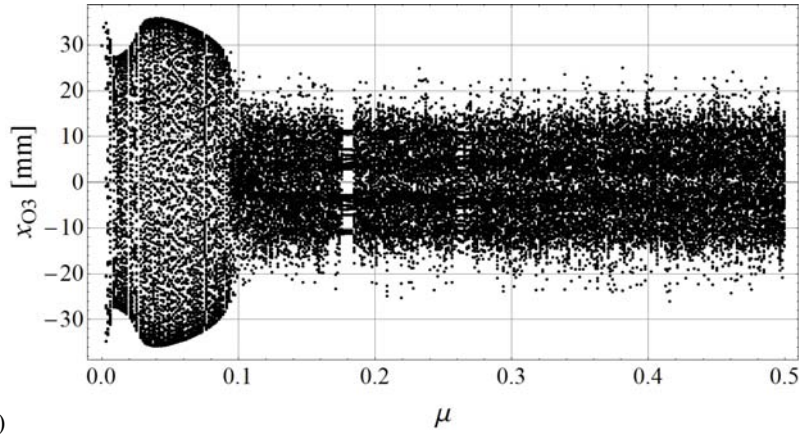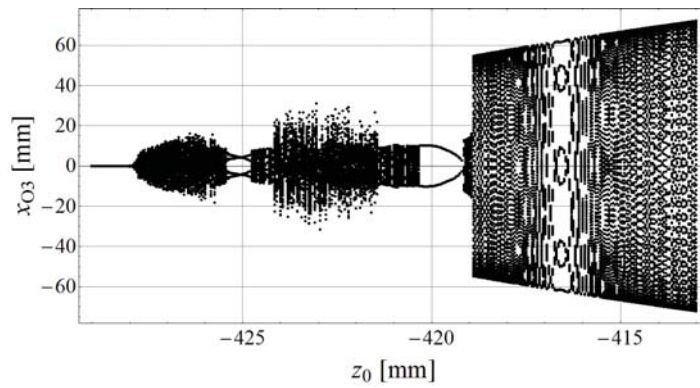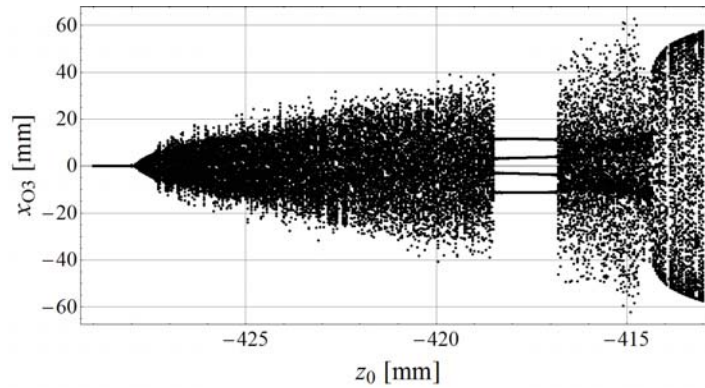
a)
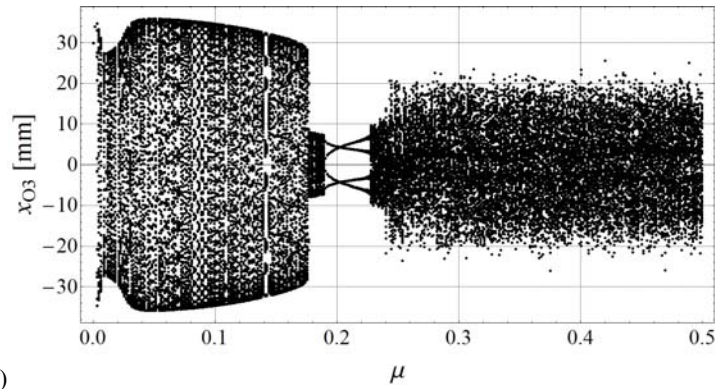
b)

Figure 4. Bifurcation diagrams of the system with friction coefficient μ as a control parameter, for $b_T = 0.681$ (a) and $b_T = 0$ (b)

Figure 5. Bifurcation diagram of the system with obstacle position z_0 as a control parameter, for

$$b_T = 0.681 .$$

a)

Figure 6. Bifurcation diagram of the system with obstacle position z_0 as a control parameter, for

$$b_T = 0$$

4. Conclusions

In this paper, the dynamic analysis of the double spatial pendulum is presented. It consists of two limbs connected with the Cardan-Hook joints. At the end of the second limb there is a spherical end, which comes in contact with the moveable obstacle. The friction force between contacting bodies is modelled based on the previous works and experience of the authors and uses the special approximation model. The bifurcation dynamics analysis, presented in this paper, shows the differences in model's behavior, while using the special model developed by the authors and in the case of point contact and no relation between friction force and rotational relative motion of contacting bodies.

The bifurcation diagrams analysis shows that the contact pressure distribution has a significant influence on the bifurcation dynamics of the system, which proves the necessity of developing advanced models of contact forces. On the other hand, this paper presents the experimental rig, which is made to verify the results obtained by the authors during the dynamics analysis. The results found out to be promising and convincing enough to make the experimental verification, which is currently being developed by the authors**.**

References

[1] Shen, J., Sanyal, A.K., Chaturvedi, N.A., Bernstein, D., McClamroch, H. ,"Dynamics and control of a 3D pendulum" 43rd IEEE Conference on Decision and Control, Georgia, USA, December 2004, pp. 323–328.

[2] Chaturvedi, N.A., McClamroch, N.H. , "Asymptotic stabilization of the hanging equilibrium manifold of the 3D pendulum" International Journal of Robust and Nonlinear Control, 17(16), 2007, pp. 1435–1454.

[3] Ludwicki, M., Awrejcewicz, J., Kudra, G., „Spatial double physical pendulum with axial excitation: computer simulation and experimental set-up" International Journal of Dynamics and Control, *3*(1), 2015, 1–8. http://doi.org/10.1007/s40435-014-0073-x.

[4] Contensou, P., 1963, "Couplage entre frottement de glissement et de pivotement dans la téorie de la toupe", In: Ziegler H. (Ed.), Kreiselprobleme Gyrodynamic, IUTAM Symposium Celerina, Springer-Verlag, Berlin, 1962, pp. 201-216.

[5] Zhuravlev V. P., Kireenkov A.A., "Padé expansions in the two-dimensional model of Coulomb friction", Mechanics of Solids 40(2), 2005 1-10.

[6] Kudra, G., Awrejcewicz, J.,"Approximate modelling of resulting dry friction forces and rolling resistance for elliptic contact shape", European Journal of Mechanics And Solids, 42, 2013

[7] Kudra, G., Awrejcewicz, J., "Application and experimental validation of new computational models of friction forces and rolling resistance", Acta Mechanica, 226(9) (2015), 2831-2848.

[8] Kudra, G., Szewc, M., Wojtunik, I., Awrejcewicz, J., „Shaping the trajectory of the billiard ball with approximations of the resultant contact forces", Mechatronics, 37, 2016, pp. 54–62. http://doi.org/10.1016/j.mechatronics.2016.01.002.

[9] Kudra, G., Szewc, M., Wojtunik, I., Awrejcewicz, J., "On some approximations of the resultant contact forces and their application in rigid body dynamics", Mechanical Systems and Signal Processing, 79, 2016, pp. 182–191.

[10] Awrejcewicz, J., and Kudra, G. Modelling and simulation of bifurcation dynamics of spatial double pendulum with rigid limiter of motion. Proceedings of the International Conference on Structural Engineering Dynamics (ICEDYN 2017), Ericeria, Portugal, July 3-5 (2017), 10 pages.

[11] Gilardi, G., Sharf, I., "Literature survey of contact dynamics modelling. Mechanism and Machine Theory", 37(10), 2012, pp.1213–1239. http://doi.org/10.1016/S0094-114X(02)00045-9.

Kudra Grzegorz, Associate Professor: Lodz University of Technology, Department of Automation, Biomechanics and Mechatronics, Stefanowskiego 1/15, 90-924 Lodz, Poland (*grzegorz.kudra@p.lodz.pl*).

Szewc Michał, Ph.D. Student: Lodz University of Technology, Department of Automation, Biomechanics and Mechatronics, Stefanowskiego 1/15, 90-924 Lodz, Poland (*michal.szewc@dokt.p.lodz.pl*), the author presented this contribution at the conference.

Ludwicki Michał, Ph.D.: Lodz University of Technology, Department of Automation, Biomechanics and Mechatronics, Stefanowskiego 1/15, 90-924 Lodz, Poland (*michal.ludwicki@p.lodz.pl*).

Witkowski Krzysztof, Ph.D. Student: Lodz University of Technology, Department of Automation, Biomechanics and Mechatronics, Stefanowskiego 1/15, 90-924 Lodz, Poland (*Krzysztof.witkowski@dokt.p.lodz.pl*).

Awrejcewicz Jan, Professor.: Lodz University of Technology, Department of Automation, Biomechanics and Mechatronics, Stefanowskiego 1/15, 90-924 Lodz, Poland (*jan.awrejcewicz@p.lodz.pl*).